



Provided by the author(s) and University of Galway in accordance with publisher policies. Please cite the published version when available.

Title	The mechano-sorptive creep behaviour of basalt FRP reinforced timber elements in a variable climate
Author(s)	O'Ceallaigh, Conan; Sikora, Karol; McPolin, Daniel; Harte, Annette M.
Publication Date	2019-09-25
Publication Information	O'Ceallaigh, Conan, Sikora, Karol, McPolin, Daniel, & Harte, Annette M. (2019). The mechano-sorptive creep behaviour of basalt FRP reinforced timber elements in a variable climate. <i>Engineering Structures</i> , 200, 109702. doi: https://doi.org/10.1016/j.engstruct.2019.109702
Publisher	Elsevier
Link to publisher's version	https://doi.org/10.1016/j.engstruct.2019.109702
Item record	http://hdl.handle.net/10379/15509
DOI	http://dx.doi.org/10.1016/j.engstruct.2019.109702

Downloaded 2024-04-27T09:11:54Z

Some rights reserved. For more information, please see the item record link above.



The Mechano-sorptive Creep Behaviour of Basalt FRP Reinforced Timber Elements in a Variable Climate

Conan O’Cearlaigh^{1,*}, Karol Sikora², Daniel McPolin³, Annette M. Harte¹

¹ College of Engineering & Informatics, National University of Ireland Galway, University Rd., Galway, Ireland

² Faculty of Engineering and Information Sciences, University of Wollongong in Dubai, UAE

³ School of Planning, Architecture and Civil Engineering, Queen’s University Belfast, University Road, Belfast BT7 1NN, UK

Email: conan.ocarlaigh@nuigalway.ie*, karolsikora@uowdubai.ac.ae, d.mcpolin@qub.ac.uk, annette.harte@nuigalway.ie

Highlights

- A significant reduction in total creep deflection is observed in FRP reinforced beams.
- Reduction in total creep strain observed on the tension face due to FRP reinforcement.
- Reduced creep deflection cannot be attributed to reduced mechano-sorptive creep behaviour.
- The restrained hygro-mechanical behaviour results in reduced creep deflection.

ABSTRACT: The use of Fibre Reinforced Polymer (FRP) reinforcement has been shown to improve the short-term flexural behaviour of timber elements. This is particularly important when reinforced elements are subjected to a variable climate condition, which is known to accelerate long-term or creep behaviour. In this paper, both unreinforced and Basalt FRP reinforced beams are subjected to creep tests at a common maximum compressive stress of 8 MPa over a 75-week period. Results demonstrated a significant reduction in total creep deflection due to the FRP reinforcement. Using matched groups, experimentally measured total strain behaviour is decomposed into the elastic, viscoelastic, mechano-sorptive and swelling/shrinkage strain components. Analysis has shown that the mechano-sorptive component is similar in unreinforced and reinforced beams. The reduction in creep behaviour of the reinforced members was primarily due to the restrained swelling/shrinkage response of the reinforced beams and was independent of the mechano-sorptive effect. This finding demonstrates the positive influence of FRP reinforcement on the long-term behaviour of timber elements and indicates a potential to describe the long-term deflection performance of FRP reinforced elements from short-term swelling/shrinkage tests.

KEYWORDS: basalt fibre; engineered wood products; mechano-sorptive creep; reinforced timber; Sitka spruce; swelling and shrinkage; viscoelastic creep.

31 1 Introduction

32 In recent times, FRP (Fibre Reinforced Polymer) materials have been increasingly used to strengthen and stiffen structural
33 timber products. Across Europe, this technology has been used, not only in new structures, but in the upgrading and repair
34 of existing structures [1,2]. When retrofitting these structures, changes in use of the building or, indeed, changes in building
35 regulations often require a higher load capacity than that of the existing members. The additional capacity requirements
36 can be successfully achieved in a timely and cost-effective manner through the use of FRP reinforcement [1–15]. More
37 widespread use of this technology has been hampered by the lack of a harmonised standard governing their design.
38 Currently, design rules for FRP reinforcement are not included in Eurocode 5 [16]. This is partly due to a lack of knowledge,
39 particularly related to the long-term behaviour.

40 In timber structures, when stressed under load, the initial elastic response is followed by viscoelastic behaviour with time.
41 Viscoelastic creep is the deformation with time at constant stress under constant environmental conditions. Due to the
42 hygroscopic nature of timber, additional effects must be considered when the relative humidity of the surrounding
43 environment fluctuates, namely, mechano-sorptive and swelling/shrinkage behaviour. Minimisation of the long-term
44 deformation is key to efficient design as this is often the controlling factor in the design of timber structures, particularly
45 in variable climatic conditions.

46 The total strain (ϵ_T), experienced by a timber element in a variable climate may be written as

$$\epsilon_T = \epsilon_e + \epsilon_{ve} + \epsilon_{ms} + \epsilon_s \quad (1)$$

47 where ϵ_e = elastic strain, ϵ_{ve} = viscoelastic strain, ϵ_{ms} = mechano-sorptive strain, ϵ_s = swelling/shrinkage strain.

49 Due to the complex nature of timber, quantifying creep, both viscoelastic and mechano-sorptive, can be difficult. Several
50 investigators have shown that viscoelastic creep rates increase with increasing stress [17,18], temperature [19] and moisture
51 content [20]. The use of FRP reinforcement has been shown to be effective in enhancing the viscoelastic behaviour of
52 timber elements under the same load level [21–24]. O’Ceallaigh et al. [24] showed that this reduction in viscoelastic creep
53 can be attributed to the enhanced flexural stiffness of the reinforced beams.

54 Mechano-sorptive creep in solid and engineered wood products loaded at different stress levels and subjected to different
55 relative humidity cycles has been investigated by several authors [25–36]. Researchers have also examined the effect of a
56 range of variables on mechano-sorptive creep. Bengtsson [37] monitored the influence of several material parameters on
57 mechano-sorptive creep in Norway spruce beams and found that relative creep was most strongly related with the elastic
58 modulus. Armstrong [25] has shown that the greater the moisture differential in each relative humidity cycle, the greater
59 the magnitude of creep. Abdul-Wahab et al. [38] performed long-term creep tests on 65 unreinforced glued laminated and
60 solid timber beam specimens under three sets of environmental conditions over an eight-year period. These conditions

61 happened to coincide with Service Classes 1, 2 and 3 as defined in Eurocode 5 [16]. They found that beams where the
62 relative humidity (RH) was cycled between 30% and 100% displayed a 285% increase in creep compared to beams tested
63 at a constant RH of 60%. When cycling between 30% and 70%, the corresponding increase was 165%.

64 While the mechano-sorptive creep of timber has been the subject of many studies, this behaviour in reinforced timber
65 members has received less attention. Some of the more relevant studies were performed by Gilfillan et al. [39] and Kliger
66 et al. [40]. In an external but sheltered climate, Gilfillan et al. [39] performed creep tests on an equal proportion of
67 unreinforced control beams and beams reinforced with carbon fibre reinforced polymer (CFRP). As only three beams of
68 each type were tested, it was not possible to draw any significant conclusions; however, a reduced total creep deflection
69 was recorded in the reinforced beams. In Kliger et al. [40], a total of 24 beams measuring 45 x 70 x 1100 mm³ were
70 manufactured. Four groups, equal in terms of elastic modulus were created, and three of these groups were reinforced with
71 a different reinforcing material in the tension zone. The three reinforcement schemes involved the adhering of either CFRP
72 or steel plates in grooves routed the entire length of the beams. Each beam was loaded in four-point bending to a common
73 maximum compressive bending stress in the timber of 8 MPa. The climate was cycled between 30% and 90% relative
74 humidity in a 28 day cycle while the temperature remained constant at 23°C for the duration of the test. The results indicate
75 that the addition of approximately 2% area reinforcement of CFRP reinforcement not only improves the short-term flexural
76 performance of the beam but also reduces the long-term mechano-sorptive creep deflection so that it is possible to increase
77 the span length by as much as 20% compared to unreinforced beams. It must be noted that in this study, the total creep was
78 measured without distinguishing between the viscoelastic (ϵ_{ve}), mechano-sorptive (ϵ_{ms}) and swelling/shrinkage (ϵ_s)
79 behaviour so the influence of the reinforcement on the mechano-sorptive component of the response cannot be quantified.

80 1.1 Objectives of the Current Study

81 The objective of the current study is to investigate the influence of near surface mounted (NSM) flexural FRP reinforcement
82 on the long-term behaviour of structural timber beams in a variable climate. To develop models to predict long-term
83 responses requires that the influence of reinforcement on each component of the response is characterised. This requires
84 the decomposition of the total strain into the elastic, viscoelastic, mechano-sorptive and swelling/shrinkage components.
85 The elastic strain (ϵ_e) and viscoelastic strain (ϵ_{ve}) have been previously characterised by O’Cearraigh et al. [24] by testing
86 matched groups in a constant climate. Their results have shown that there is a statistically insignificant difference in the
87 creep deflection behaviour of unreinforced and reinforced beams in a constant climate condition. The current study focuses
88 on characterising the total strain (ϵ_T) behaviour and swelling/shrinkage strain (ϵ_s) behaviour in a variable climate. From
89 this, the mechano-sorptive (ϵ_{ms}) component of the unreinforced and reinforced beams is determined using Equation (2).

$$\varepsilon_{ms} = \varepsilon_T - (\varepsilon_e + \varepsilon_{ve} + \varepsilon_s) \quad (2)$$

90 The experimental programme has been specifically designed to minimise the influence of timber variability and stress level
91 on the response so that the influence of the FRP reinforcement can be isolated. The knowledge gathered in this study will
92 contribute to the future development of design guidelines for reinforced timber elements.
93

94 2 Experimental Programme

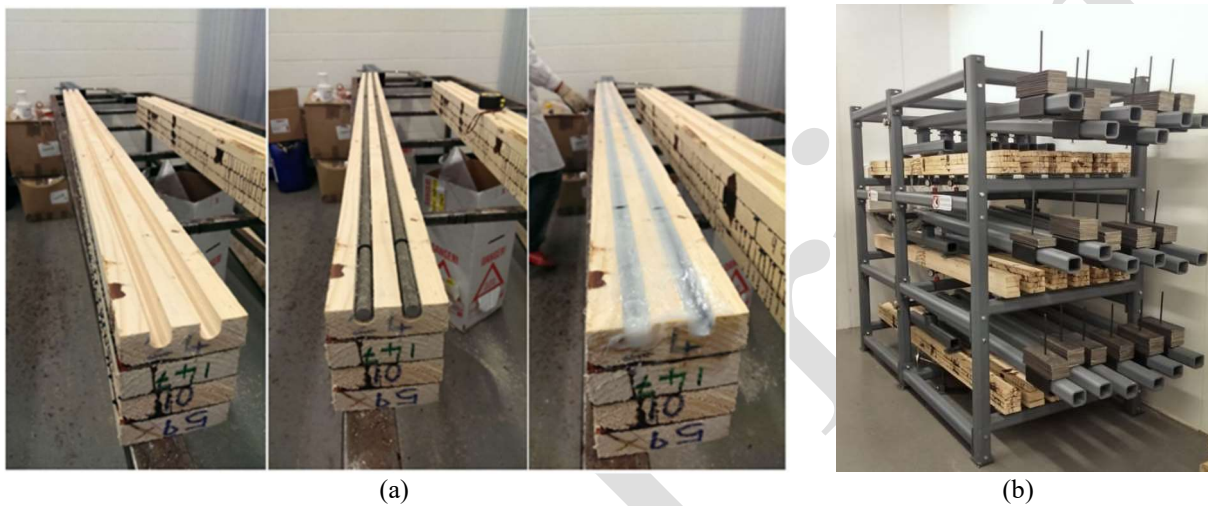
95 2.1 Introduction

96 The test programme is designed to enable the elastic, viscoelastic, mechano-sorptive and swelling/shrinkage components
97 of unreinforced and reinforced beams to be individually characterised so that the influence of the FRP reinforcement can
98 be determined.

99 2.2 Materials and Methods

100 The timber used in this study was grade C16 Sitka spruce [41]. Forty glulam beams, comprising four laminations and
101 measuring approximately 98 mm x 125 mm x 2300 mm, were designed and manufactured. Short-term flexural testing in
102 accordance with EN 408 [42] was performed on all beams and statistical methods were utilised to create five matched
103 groups equal in terms of mean flexural stiffness. Using matched groups helps to minimise the differences in responses
104 arising from the natural variability in timber properties. The statistical tests involved Shapiro-Wilk test and Levene's test
105 to assess normality of the samples and homogeneity of the group variances, respectively. Depending on the results of the
106 Shapiro-Wilk tests and Levene's test, either a Student's t-test or modified Student's t-test (Welch's t-test) was carried out
107 to compare the means of each group to one another. The results showed no statistical evidence to suggest that the mean of
108 any group is not equal to any other group in their unreinforced state. Subsequently, twenty of the beams were reinforced
109 with two, 12 mm diameter basalt fibre reinforced polymer (BFRP) rods inserted into routed grooves along the bottom
110 tensile lamination as seen in **Fig. 1(a)**. This corresponds to a mean reinforcement area of 1.85% of the beam cross-sectional
111 area. The grooves were centred 30 mm from each side of the beam and sized to include the BFRP rods plus a 2 mm epoxy
112 glue-line. The adhesive used was a two-part thixotropic structural epoxy specially formulated for bonding of FRP to timber.
113 To ensure the correct glue-line thickness was achieved, 2 mm rubber rings were placed at 300 mm centres along the length
114 of the BFRP rod. Once reinforced, the ends and the bottom face of each beam in the test programme were coated with a
115 waterproof varnish to ensure both unreinforced and reinforced specimens are subjected to common exposure conditions in
116 the variable climate.

117 The BFRP rods used were reported by the manufacturers to have a modulus of elasticity of $45000 + \text{N/mm}^2$ and a tensile
118 strength of $1000 + \text{N/mm}^2$ [43]. Experimental tests in accordance with ISO 10406-1 [44] gave a mean modulus of elasticity
119 of 50700 N/mm^2 and a mean tensile strength of 905 N/mm^2 for the batch used in this study [45]. Creep tests on the BFRP
120 rods were carried out at stress levels of 3.85%, 8% and 15% of the ultimate tensile strength using the same standard [42].
121 The theoretical stress level in the BFRP rods in the loaded experimental beams in this study is 3.85%. The results showed
122 that the creep of the BFRP rods was negligible at all stress levels tested with a maximum creep strain of only $25 \mu\epsilon$ occurring
123 at a stress level of 15%.



124
125

126 **Fig. 1.** Reinforced beams: (a) Manufacture of reinforced members, (b) 18 beams loaded in the creep test frame

127
128

To characterise the influence of the reinforcement on the total creep response of timber elements, two matched groups (one
129 unreinforced and one reinforced), comprising nine beams each, were subjected to long-term creep testing in a variable
130 climate condition. These are referred to as “Group UV” (UV = Unreinforced Variable Climate) and “Group RV” (RV =
131 Reinforced Variable Climate). The beams were initially conditioned in a constant climate at a relative humidity of $65 \pm 5\%$
132 and at a temperature of $20 \pm 2^\circ\text{C}$ prior to testing. Each beam was loaded under four-point bending in the creep test frame
133 to a common maximum compression bending stress of 8 MPa. The magnitude of the bending stress is greater than that
134 typically experienced by an in-service timber element [46] but was chosen to produce measurable creep deformations in a
135 reasonable period without causing failure of the member. This common compressive bending stress produces a similar
136 stress distribution in both unreinforced and reinforced beams but also means that different loads must be applied to the
137 unreinforced and reinforced members. Mean vertical loads of approximately 6241 N and 5748 N were applied via a lever
138 arm mechanism to the reinforced and unreinforced beams, respectively [24]. The mid-span vertical deflection was
139 monitored throughout using Mitutoyo displacement dial gauges with an accuracy of 0.01 mm. The initial elastic deflection
140 of both unreinforced and reinforced beams was shown to be in good agreement with the predicted deflection based on a
141 linear elastic model. The long-term vertical deflection test results are monitored relative to the supports and expressed in

142 terms of both total deflection and relative creep (C_R) deflection, which is defined as the deflection at time t , expressed as a
143 proportion of the initial elastic deflection as seen in Equation (3) [29].

$$C_R(t) = \frac{w(t)}{w_0} \quad (3)$$

144 where C_R = relative creep, w_0 = initial deflection defined as the deflection 60 seconds after the load was applied and $w(t)$
145 = deflection at time t .

146 The mid-span longitudinal strain is measured using electrical resistance strain (ERS) gauges (TML type PLW-60-11) on
147 the compression and tension faces as seen in **Fig. 2**. The initial elastic strain agreed with predicted elastic strain behaviour
148 of beams subjected to a maximum compressive stress of 8 MPa. The ERS strain gauges, specifically designed for long-
149 term measurements on low modulus materials such as wood, measure a change in the electrical resistance of the gauge
150 which is correlated to strain. The ERS gauge length of 60 mm was chosen to overcome some of the inherent variability of
151 timber. Natural defects can potentially result in poor strain measurement when using smaller strain gauges. A gauge length
152 of 60 mm is less influenced by small defects and provides a better representation of the strain on the timber surface.

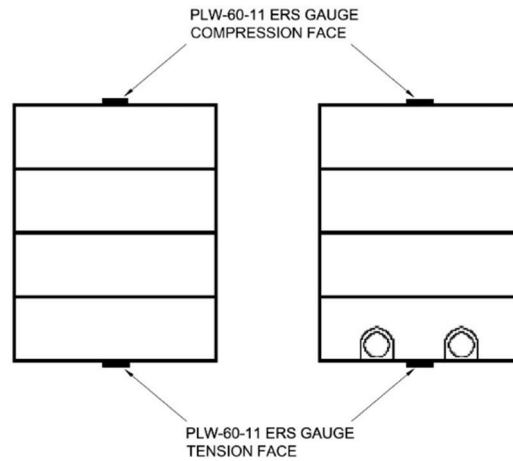
153 In the same variable climate, the hygro-expansion or swelling/shrinkage (ϵ_s) strain components are measured on non-loaded
154 beams. These beams known as “Group MC” (MC = Moisture Content), are used to measure the swelling/shrinkage
155 behaviour of the timber in a non-loaded state. This group is one of the five groups which was matched based on the flexural
156 stiffness. This group comprised four specimens measuring 98 x 125 x 1000 mm³. Each beam is monitored with ERS gauges
157 aligned in the longitudinal direction on the top and bottom faces as seen in **Fig. 2a** and **Fig. 2b**. The longitudinal strain
158 measured on the top and bottom face of each beam represent the moisture-induced swelling/shrinkage strain component
159 that would occur on the compression and the tension face of the loaded creep test specimens, respectively [47]. For this
160 reason, the bottom face is referred to as the tension face and the top face is referred to as the compression face. The
161 specimens were supported at 250 mm centres on low-friction polytetrafluorethylene (PTFE) plates to allow free swelling
162 and shrinkage of each specimen and minimise strains due to self-weight [47].

163 Further tests were performed on the BFRP rods to examine their swelling/shrinkage behaviour. Swelling and shrinkage
164 tests demonstrated that the BFRP rod reinforcement was dimensionally stable when subjected to the same variable climate
165 as the beams [45]. There was no appreciable lateral or longitudinal expansion or increase in moisture content observed. It
166 is believed that the epoxy resin used during the manufacture to bind BFRP fibres impedes the flow of moisture and provides
167 a stable material under cyclic relative humidity conditions.

168



a)

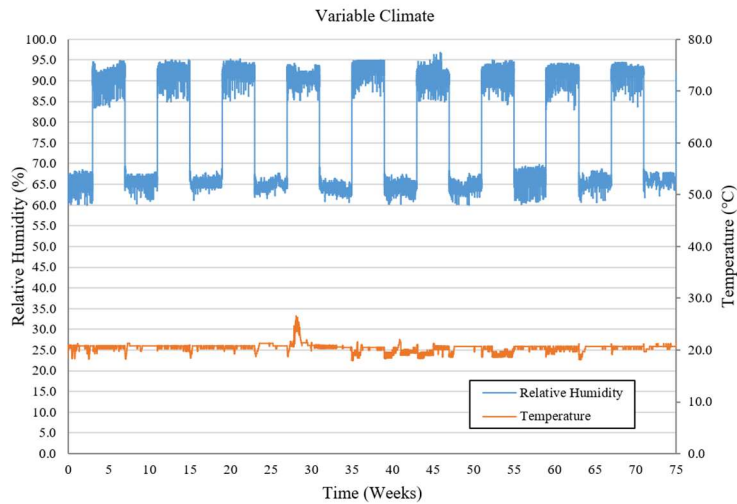


b)

Fig. 2. PLW-60-11 ERS gauge, a) PLW-60-11 ERS gauge alignment, b) PLW-60-11 ERS gauge positions on the tension and compression face of the unreinforced and reinforced beams.

2.3 Variable Climate Conditions

The variable climate condition induces mechano-sorptive creep in the loaded beams together with swelling/shrinkage strains due to hygro-expansion. This occurs due to the change in the relative humidity and subsequent change in the moisture content of the beams. A relative humidity cycle length of eight weeks (four weeks at 90% RH and four weeks at 65% RH) was implemented over a 75-week test period. This relative humidity cycle differential and length were chosen to implement a significant moisture content change throughout the cross-section of each beam in each relative humidity cycle [2]. Testing commenced at a relative humidity of $65 \pm 5\%$ and at a temperature of $20 \pm 2^\circ\text{C}$ for a period of three weeks, after which, the relative humidity in the variable climate chamber was changed to $90\% \pm 5\%$. The high relative humidity was maintained for a period of four-weeks when it was reduced to $65 \pm 5\%$ for another four weeks. It was considered beneficial to delay cycling the relative humidity for the first three weeks to observe the relatively rapid viscoelastic movement in the earlier stages of the creep test. The recorded relative humidity and temperature data can be seen in **Fig. 3**. The small abnormality within the temperature data at 28 weeks can be attributed to a thermostat failure in the conditioning chamber resulting in variations from the set constant temperature of $20^\circ\text{C} \pm 2^\circ\text{C}$.



188
189 **Fig. 3.** Relative humidity and temperature data recorded in the variable climate chamber.

190 3 Experimental Test Results

191 The creep deflection and longitudinal strain results for the unreinforced (Group UV) and reinforced (Group RV) beams
192 subjected to a variable relative humidity are presented together with the longitudinal swelling/shrinkage strain
193 measurements for the unloaded Group MC. The mean mechano-sorptive strain component of the two groups are compared
194 to examine the influence of the FRP reinforcement.

195 3.1 Long-term Deflection Results

196 The beam group, Group UV, consists of unreinforced beams loaded to a maximum compression bending stress of 8 MPa
197 in four-point bending. Eight of these beams are monitored with vertical displacement dial gauges. The deflection results
198 for these beams over the 75-week test period can be seen in **Fig. 4**. A large increase in the total deformation due to the
199 variable relative humidity is found. The mid-span deflection of the similarly stressed beams in Group RV can be seen in
200 **Fig. 5**. When compared to the deflection results of Group UV, the total deflection of the Group RV is significantly lower
201 and is more consistent with reduced variation over the 75-week test period. The reduced variation in the deflection of
202 Group RV is to be expected as defects or abnormalities, which naturally occur in timber, are reinforced and are less
203 influential on the overall deflection resulting in more consistent deflection behaviour. There is a trend of slowly increasing
204 deflection with each moisture cycle in both groups. Typically, there is an increase in the deflection during each drying
205 phase and a decrease in deflection during the wetting phase. The exception to this occurs during the first cycle where the
206 moisture content increases to a level not previously attained (Week 3-Week 7), and a significant increase in deflection was
207 recorded during a wetting phase. This behaviour has been previously observed in creep testing of timber products in
208 variable climates [33]. The magnitude of the increase is more pronounced in the unreinforced beams than in the reinforced
209 beams.

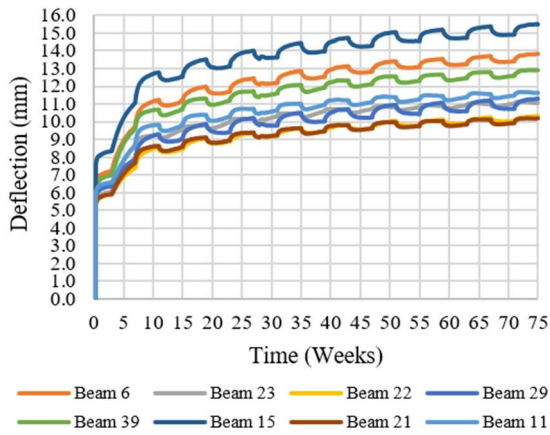


Fig. 4. Group UV mid-span deflection (mm) results.

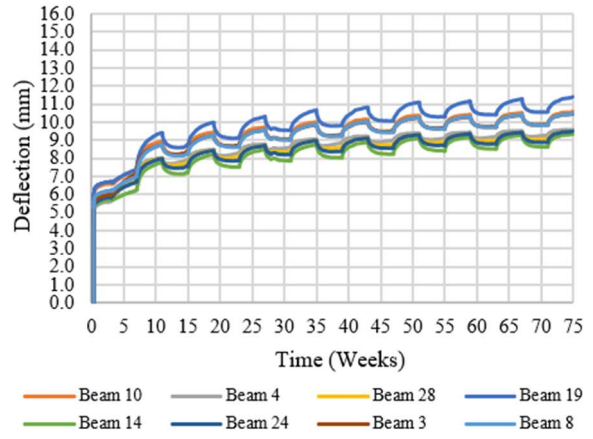


Fig. 5. Group RV mid-span deflection (mm) results.

211

212

213

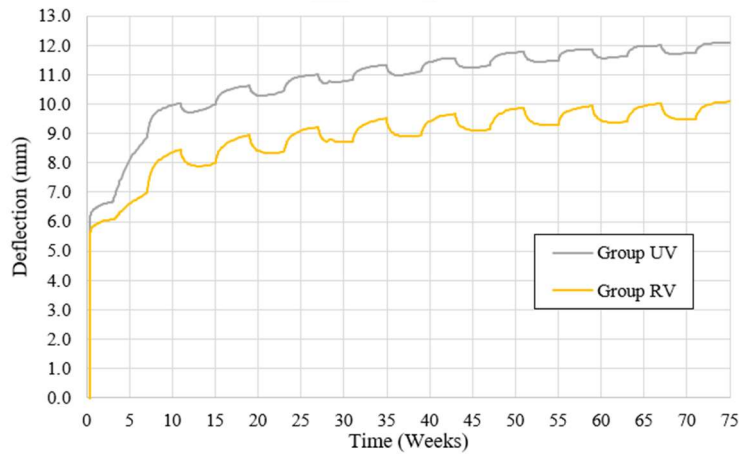
214

215

216

217

To compare the effect of the reinforcement on the long-term deflection, the mean total deflection of Group UV and Group RV are plotted together in Fig. 6. There is a significant difference between the initial elastic deflection (8.9%) of both groups due to the increased stiffness of the Group RV, as expected. This difference between the two groups increases during the first relative humidity cycle change (Week 3-Week 7) where the humidity changes from 65% ± 5% to 90% ± 5%. With additional cycles, the percentage difference continues to increase up to a maximum of 17.9% after 75 weeks with a maximum mean deflection of 12.09 mm and 10.10 mm in Group UV and the Group RV, respectively.



218

219

Fig. 6. Comparison between the unreinforced and reinforced group mean deflection results (mm) over a 75-week test period.

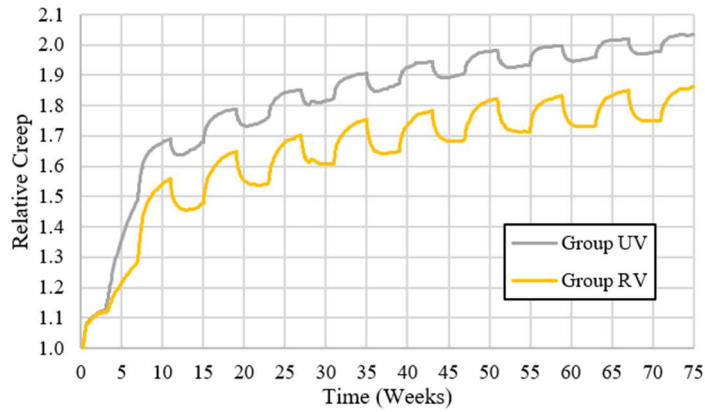


Fig. 7. Comparison between the unreinforced and reinforced group mean relative creep results over a 75-week test period.

Fig. 7 presents the average relative creep deflection results of the unreinforced and reinforced beam groups. When comparing the mean results for both groups, the unreinforced beams are found to be affected by moisture cycling to a greater extent than the reinforced beams. As seen when examining the total deflection results of these groups, the first change in relative humidity has a significant effect on the behaviour of both groups. Interestingly, the reinforced beams experience greater mean creep fluctuations with each relative humidity cycle. This was also observed by Kliger et al. [40]. This is perhaps due to an increased ability to recover creep deflection due to the addition of the reinforcement or an effect of the differential swelling/shrinkage on the tension face of reinforced beams.

To further assess the differences in responses, statistical Student's t-tests were performed at a series of time points shown in **Table 1**. In this study, all statistical tests are carried out to a significance level of 0.95 ($\alpha = 0.05$). The results show that there is no statically significant difference between Group UV and Group RV up until week 3. However, after the first complete relative humidity cycle at week 11, a statically significant difference of 8.2% exists between the relative creep deflection of Group UV and Group RV. The difference remains statistically significant throughout the remainder of the test period demonstrating the beneficial influence of the reinforcement in reducing the creep deflections. The percentage difference between the two groups increased with time to a maximum of 8.8% after 75 weeks.

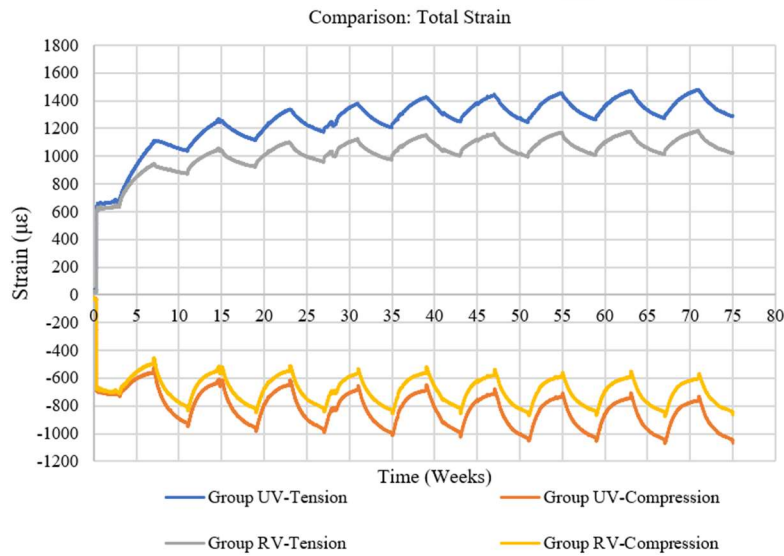
Table 1. Comparison between the mean (standard deviation) relative creep deflection of Group UV and Group RV at a series of time points throughout the test.

Relative Creep	Week 0	Week 3	Week 11	Week 19	Week 35	Week 51	Week 75
Group UV	1.004 (0.017)	1.126 (0.010)	1.682 (0.053)	1.788 (0.059)	1.906 (0.070)	1.981 (0.075)	2.034 (0.082)
Group RV	1.004 (0.012)	1.122 (0.010)	1.549 (0.035)	1.647 (0.039)	1.756 (0.044)	1.822 (0.046)	1.862 (0.048)
Percentage Diff.	0.0%	0.4%	8.2%	8.2%	8.2%	8.4%	8.8%
Student's t-test	Not Sig.	Not Sig.	Sig.	Sig.	Sig.	Sig.	Sig.
p-Value	0.9881	0.3786	0.0000	0.0001	0.0001	0.0002	0.0002

3.2 Long-term Strain Results

The longitudinal strains were measured on the tension and compression faces of seven unreinforced and seven reinforced beams using ERS gauges designed for long-term use on timber. The mean longitudinal strain results are presented in **Fig.**

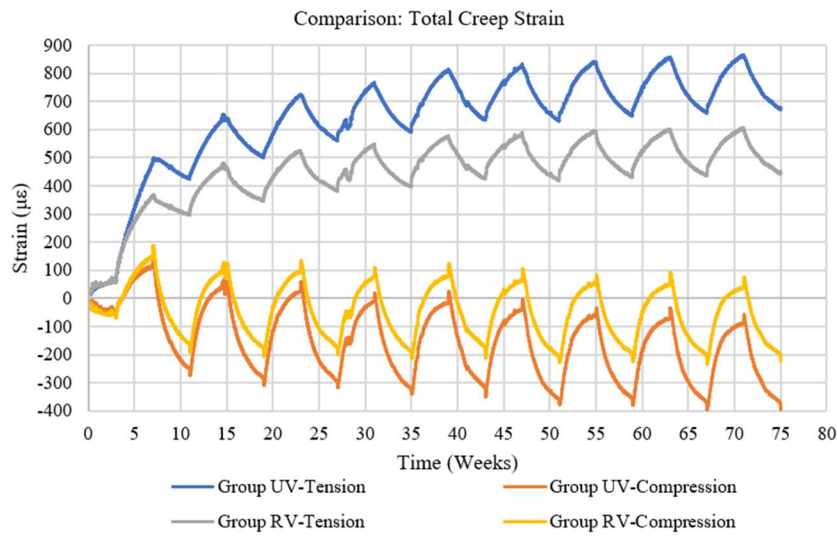
242 8. Similar mean elastic strain was observed in both groups on both faces after the initial loading as seen at time $t = 0$ in
 243 **Fig. 8**. On the tension face, mean elastic strain values of $614.6 \mu\epsilon$ and $577.3 \mu\epsilon$ were observed for Group UV and Group
 244 RV, respectively. This difference was found to be statistically insignificant. The difference in the mean elastic strain on the
 245 compression face ($-708.0 \mu\epsilon$ and $642.6 \mu\epsilon$ for Group UV and Group RV, respectively) was also found to be statistically
 246 insignificant. During the first three weeks of the creep test, the climate remained constant at $65\% \pm 5\%$ relative humidity
 247 and there was a slight increase in longitudinal strain due to viscoelastic creep. After this period, the relative humidity was
 248 increased and significant changes in longitudinal strain on the tension and compression face were observed. In **Fig. 8**, the
 249 mean total longitudinal strain (ϵ_T) on the tension face of the unreinforced group is seen to be larger than that of the
 250 reinforced group over the 75-week test period, with the largest changes seen during the first moisture content change. On
 251 the compression face, the unreinforced group experienced greater mean longitudinal strain over the entire test duration
 252 when compared to the reinforced group.



253
 254 **Fig. 8.** Mean total longitudinal strain on the tension and compression faces of Group UV and Group RV ($\epsilon_T = \epsilon_e + \epsilon_{ve} + \epsilon_{ms} + \epsilon_s$).

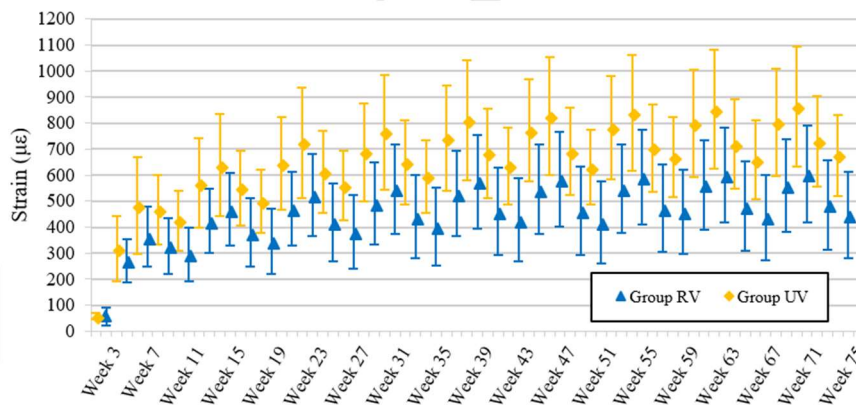
255 To solely examine the creep strain (ϵ_{creep}) component, the elastic strain component has been subtracted from the individual
 256 total strain (ϵ_T) results for each beam and the mean of these total creep strain results are presented in **Fig. 9**. During the
 257 first three weeks, similar total creep behaviour is seen on the tension and compression faces of both beam groups. Once
 258 the relative humidity is increased, significant increases in strain are observed immediately as mechano-sorptive creep
 259 effects and swelling/shrinkage strains occur. During weeks 3-7, there was a significant increase in strain as a result of the
 260 combined mechano-sorptive creep component and the swelling component as the moisture content increases. During weeks
 261 7-11, there was a reduction in the strain measured in each case as the relative humidity reverted to $65\% \pm 5\%$ and the

262 moisture content decreased. As the relative humidity cycling continued, it can be seen that on both the tension and
 263 compression face, the Group UV experience greater mean total creep strain.
 264



265
 266 **Fig. 9.** Mean longitudinal creep strain on the tension and compression faces of Group UV and Group RV ($\epsilon_{creep} = \epsilon_{ve} + \epsilon_{ms} + \epsilon_s$).

267 In **Fig. 10**, the mean total creep strains and corresponding standard deviations on the tension side of both Group UV and
 268 Group RV can be seen at a series of time points. The standard deviation is plotted to compare the significance of the
 269 observed differences.



270
 271 **Fig. 10.** Mean and standard deviation of total longitudinal creep strain on the tension face ($\epsilon_{creep} = \epsilon_{ve} + \epsilon_{ms} + \epsilon_s$)
 272

273 A proportion of these time points are chosen and presented in **Table 2**. All of the points after week 3 are chosen to
 274 correspond with peak strains associated with the end of a wetting period. It can be seen that, at week 3, a statistically
 275 insignificant difference of 3.7% exists between the mean total creep strain of the two groups. While there is a large increase
 276 in the percentage difference (28.0%) after week 7 due to the first wetting cycle, the difference is not statistically significant.
 277 The total creep strain slowly increases with each subsequent cycle and the percentage difference between Group UV and
 278 Group RV continuously increases up to a maximum of 35.2% at week 71. Statistical Student's t-tests have shown that after

279 week 31 the difference becomes statistically significant and there is a beneficial reduction in total creep strain on the tension
 280 face due to the reinforcement.

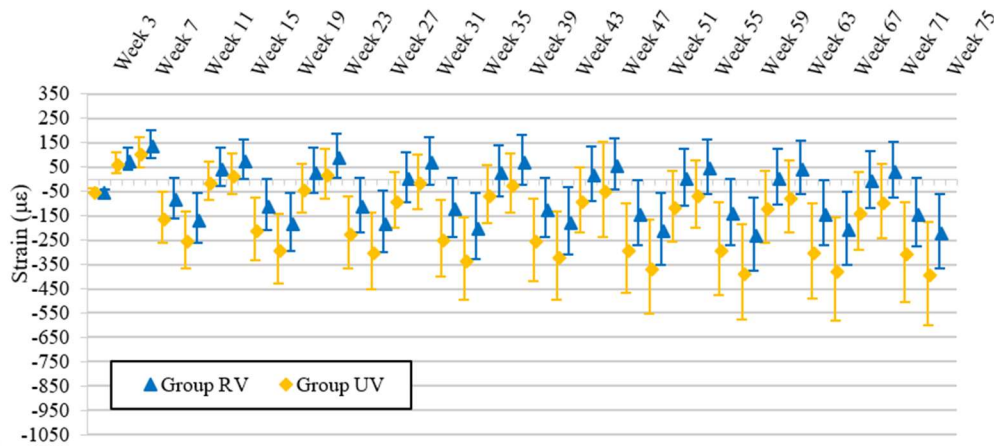
281 **Table 2.** Comparison of mean (standard deviation) total longitudinal creep strains on the tension faces of Groups UV and RV.

Strain ($\mu\epsilon$)	Week 3	Week 7	Week 15	Week 31	Week 47	Week 55	Week 71
Group UV	58.38 (13.10)	481.81 (186.50)	638.39 (195.62)	765.69 (220.12)	826.40 (226.81)	838.86 (221.02)	863.38 (229.49)
Group RV	56.26 (34.05)	363.64 (115.30)	467.53 (139.84)	546.21 (171.40)	583.22 (182.78)	591.72 (183.12)	605.18 (187.43)
Percentage Diff.	3.7%	28.0%	30.9%	33.5%	34.5%	34.6%	35.2%
Student's t-test	Not Sig.	Not Sig.	Not Sig.	Not Sig.	Sig.	Sig.	Sig.
p-Value	0.880	0.179	0.085	0.059	0.047	0.042	0.040

282

283 In **Fig. 11**, the mean total creep strains and the corresponding standard deviations on the compression faces of both the
 284 unreinforced and the reinforced groups can be seen at a series of time points. It can be seen that Group UV experiences
 285 greater total creep compression strains on average. To investigate this further, significance testing is carried out at a series
 286 of time points and results are presented in **Table 3**. After week 3, these points were chosen to correspond to the peak total
 287 creep compressive strains associated with the end of a drying period.

288



289

290 **Fig. 11.** Mean and standard deviation of total longitudinal creep strain on the compression face

291

292 **Table 3.** Comparison of mean (standard deviation) total longitudinal creep strains on the compression faces of Groups UV and RV.

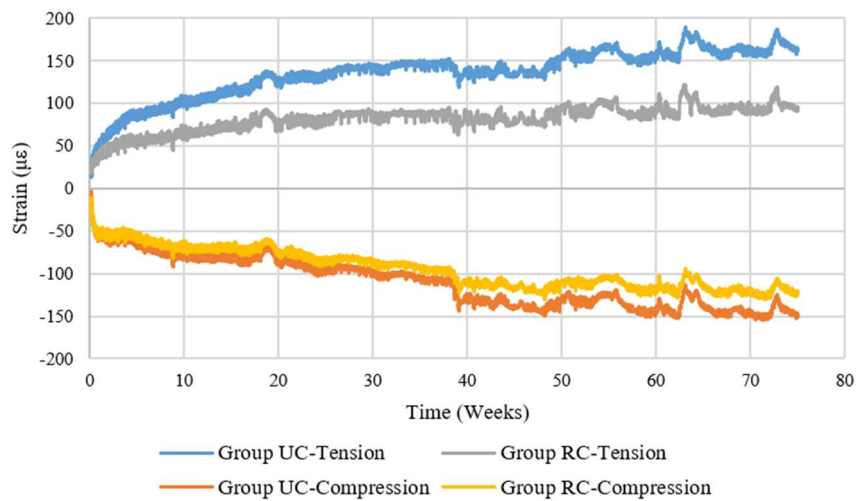
Strain ($\mu\epsilon$)	Week 3	Week 11	Week 19	Week 35	Week 51	Week 67	Week 75
Group UV	-46.19 (10.54)	-254.75 (114.54)	-285.76 (143.65)	-327.00 (169.07)	-359.75 (194.95)	-369.28 (211.52)	-386.80 (213.01)
Group RV	-59.62 (18.53)	-166.59 (101.85)	-177.53 (119.45)	-194.14 (136.35)	-204.84 (148.09)	-200.51 (150.81)	-213.78 (151.46)
Percentage Diff.	25.4%	41.9%	46.7%	51.0%	54.9%	59.2%	57.6%
Student's t-test	Not Sig.	Not Sig.	Not Sig.	Not Sig.	Not Sig.	Not Sig.	Not Sig.
p-Value	0.124	0.156	0.154	0.134	0.122	0.114	0.108

293

294 The percentage difference increases from 25.4% at week 3 to 41.9% at week 11 after the first relative humidity cycle. The
 295 percentage difference continues to increase with each cycle; however, the difference has been shown to be not statically
 296 significant.

297 3.3 Viscoelastic Strain Component

298 To characterise the viscoelastic strain behaviour (ϵ_{ve}) of unreinforced and reinforced beams, O’Ceallaigh et al. [24]
299 subjected matched groups of beams to creep testing in a constant climate condition. These groups are referred to as “Group
300 UC” (UC = Unreinforced Constant Climate) and “Group RC” (RC = Reinforced Constant Climate). The mean viscoelastic
301 creep strain on the tension and compression face of the unreinforced Group UC and the reinforced Group RC are presented
302 graphically in **Fig. 12** and further information may be found in the article [24]. The mean viscoelastic creep strain on the
303 compression face of Group UC and Group RC can be seen to be in good agreement. In contrast, on the tension face, a
304 beneficial reduction in viscoelastic creep strain can be observed in the reinforced Group RC, demonstrating the positive
305 influence of FRP reinforcement on the creep behaviour of reinforced members. It should be noted that although there was
306 a beneficial reduction in viscoelastic creep strain on the tension face, there was no statically significant reduction in creep
307 deflection over the 75-week test period.

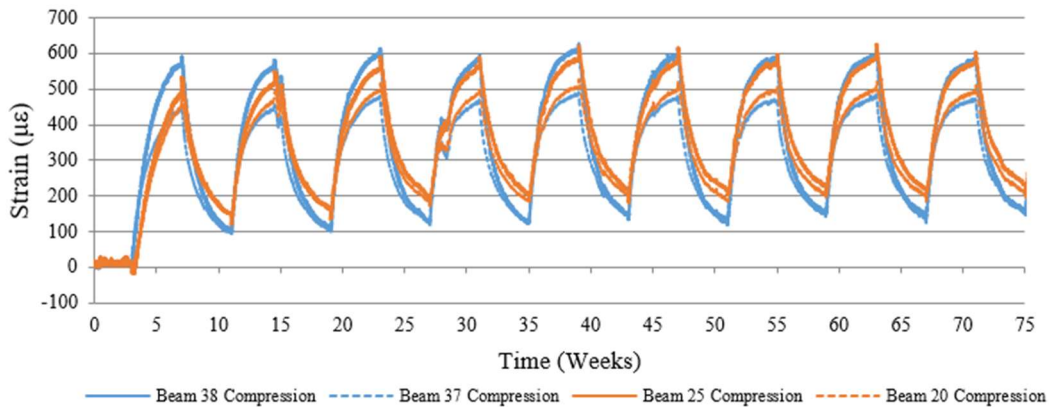


308 **Fig. 12.** Mean longitudinal viscoelastic creep strain (ϵ_{ve}) on the tension and compression faces of Group UC and Group RC.
309

310 3.4 Swelling/shrinkage Strain Component

312 To investigate the swelling/shrinkage behaviour of the unreinforced and reinforced beams, four specimens were placed
313 in the variable climate condition to monitor strains development due to changing moisture content. These beams,
314 collectively known as Group MC, comprise two reinforced beams (Beam 20 and Beam 25) and two unreinforced beams
315 (Beam 37 and Beam 38). Prior to reinforcement, this beam group had been matched in terms of bending stiffness to Group
316 UV and Group RV using statistical methods to ensure common timber material properties for each group. The beams were
317 initially conditioned to approximately 12% moisture content and placed in the variable climate presented previously in **Fig.**
318 **3.**

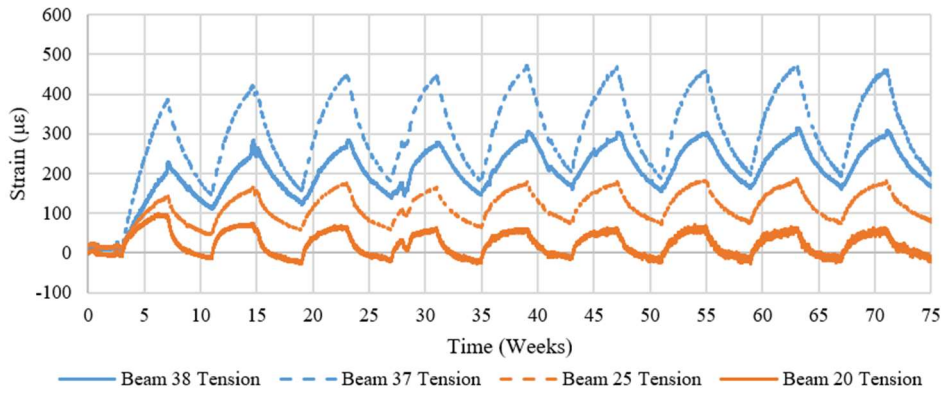
319 The strain in the longitudinal direction on the top (compression face) of the beams is shown in **Fig. 13**. The top lamination
320 is exposed to the surrounding environment on the top surface and both sides of the lamination. The measured
321 swelling/shrinkage strain in the longitudinal direction remains at approximately $0 \mu\epsilon$ for the first 3 weeks of the test as the
322 relative humidity remained constant at $65\% \pm 5\%$. After this period, the relative humidity is cycled between $65\% \pm 5\%$ and
323 $90\% \pm 5\%$.



324
325 **Fig. 13.** Swelling/shrinkage strain results (ϵ_s) on the compression face of unreinforced and reinforced beams

326 The increase in relative humidity causes a rapid increase in strain due to the increasing moisture content of the beams. The
327 opposite is seen as the relative humidity is reduced with a rapid decrease in the swelling/shrinkage strain during the
328 desorption phase of the cycle. There was negligible difference between strain measured on the compression face of the
329 unreinforced and reinforced beams as each ERS gauge is aligned along the top lamination, which is negligibly affected by
330 the reinforcement in the bottom lamination

331 The measured longitudinal strain on the bottom (tension face) of the beams can be seen in **Fig. 14**. The unreinforced
332 specimens, shown in blue, experience greater swelling/shrinkage strains in the longitudinal direction, when compared to
333 the reinforced specimens, shown in orange. As both unreinforced and reinforced beam specimens are sealed on the bottom
334 face with a waterproof varnish, moisture flow through this tensile laminate is through the sides. The position of the BFRP
335 rod reinforcement in the tension zone of the reinforced members not only provides a restraining force but also impedes
336 moisture flow and results in a reduction in the measured swelling/shrinkage strains or hygro-mechanical response of the
337 reinforced members.



338

339 **Fig. 14.** Swelling/shrinkage strain results (ϵ_s) on the tension face of unreinforced and reinforced beams.

340 To compare the swelling/shrinkage strain on the tension face of unreinforced and reinforced beams, the mean strain results
 341 are compared at a series of time points. These time points correspond to each maximum peak swelling/shrinkage strains
 342 and are tabulated in **Table 4**. There is a 24.8% difference between the strains measured on unreinforced and reinforced
 343 beams after 0 weeks; however, after the first moisture increase (Week 7), a large 85.5% difference can be seen between
 344 the swelling/shrinkage strains measured on the tension face. The percentage difference remains relatively consistent with
 345 subsequent cycles achieving percentage differences greater than 100% with a maximum of 106.0% observed at week 71.
 346 This difference is likely to be significant but due to the low sample size, statistical tests were not carried out.

347 **Table 4.** Percentage difference between mean tensile swelling/shrinkage strains (ϵ_s) observed in the unreinforced and reinforced beams
 348 in Group MC ($\mu\epsilon$).

Strain ($\mu\epsilon$)	Week 0	Week 7	Week 15	Week 31	Week 47	Week 63	Week 71
Unreinforced	10.64 (2.31)	297.20 (124.33)	327.78 (109.71)	361.29 (120.69)	384.30 (120.69)	389.32 (117.90)	384.66 (115.50)
Reinforced	8.29 (10.97)	119.26 (34.15)	107.38 (68.70)	112.97 (75.51)	119.50 (85.43)	120.10 (91.40)	118.15 (88.54)
Percentage Diff.	24.8%	85.5%	101.3%	104.7%	105.1%	105.7%	106.0%

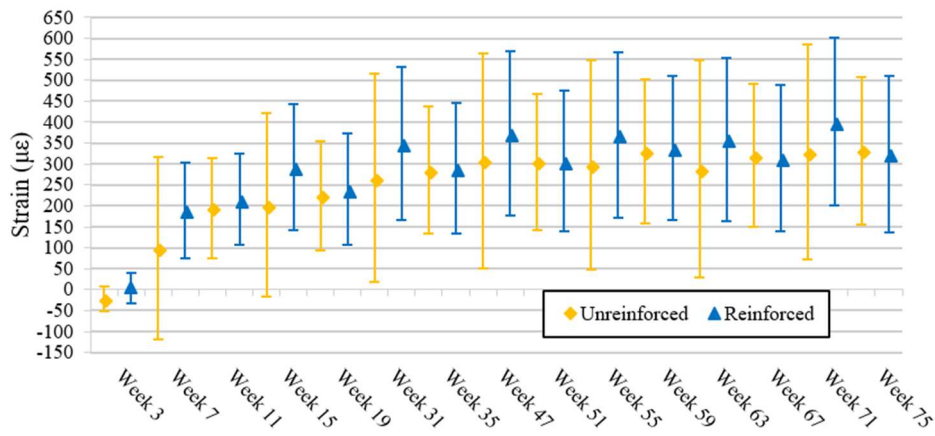
349

350 This indicates a significant reduction in strain due to the influence of the NSM reinforcement in the tension zone of the
 351 reinforced beams. This restraining behaviour is due to the greater stiffness of the BFRP rods and also their dimensional
 352 stability under moisture cycling.

353 3.5 Mechano-sorptive Creep Strain Component

354 The total creep strain may be separated into its component parts as described previously using Equation (1). Using
 355 matched groups, the mean elastic and viscoelastic strain components reported in [24] and the swelling/shrinkage strain
 356 component presented here are subtracted from the mean total strain measurements to determine the mechano-sorptive creep
 357 strain. In **Fig. 15**, the mean mechano-sorptive strain components on the tension face of the unreinforced and reinforced
 358 groups at a series of time points are presented. To calculate the standard deviation associated with the mechano-sorptive
 359 strain component, the combined variance of the measured strain components is considered in the analysis at each time

360 point. To compare the difference in the mean value of both groups, a series of statistical Student's t-tests were performed,
 361 and the results are presented in **Table 5**.



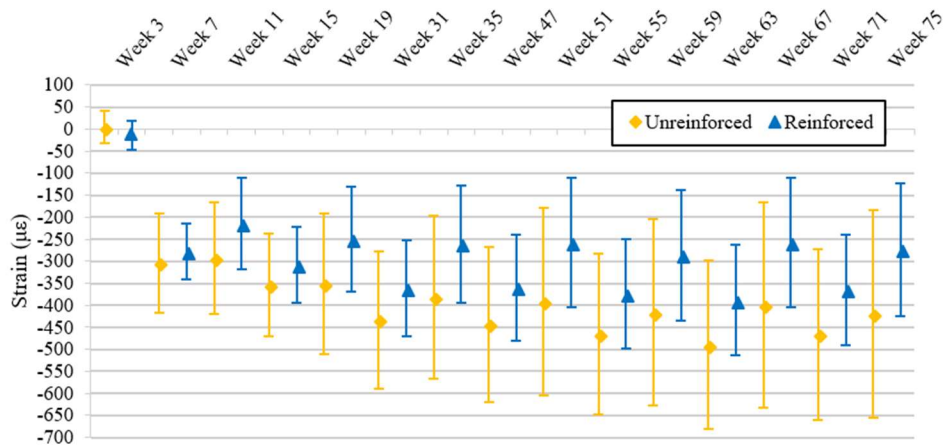
362
 363 **Fig. 15.** Mean mechano-sorptive strain (ϵ_{ms}) and associated standard deviations on the tension face of unreinforced and reinforced
 364 beams

365
 366 It can be seen that the percentage difference in mechano-sorptive creep is largest at the beginning of the test with 9.5%
 367 at week 11 compared to 2.4% at week 75. The Student's t-tests show no statistically significant differences between the
 368 means of both groups on the tension face.

369 **Table 5.** Comparison between the mean (standard deviation) mechano-sorptive strain (ϵ_{ms}) on the tension side of unreinforced and
 370 reinforced beams ($\mu\epsilon$)

Strain ($\mu\epsilon$)	Week 11	Week 19	Week 35	Week 51	Week 67	Week 75
Unreinforced	200.17 (119.42)	224.12 (129.94)	285.54 (150.96)	304.65 (161.80)	319.95 (170.87)	331.73 (176.26)
Reinforced	220.07 (108.20)	239.88 (132.46)	290.17 (156.39)	307.23 (169.00)	312.93 (174.92)	323.95 (187.34)
Percentage Diff.	9.5%	6.8%	1.6%	0.8%	2.2%	2.4%
Student's t-test	Not Sig.	Not Sig.	Not Sig.	Not Sig.	Not Sig.	Not Sig.
p-Value	0.749	0.826	0.956	0.977	0.941	0.937

371
 372 In **Fig. 16**, the mean mechano-sorptive strain and associated standard deviations on the compression face of the
 373 unreinforced and reinforced beams are plotted at a series of time points. There appears to be slightly greater mechano-
 374 sorptive creep strain on the Group UV when compared to Group RV. To examine this further, statistical Student's t-tests
 375 were performed and a series of these are presented in **Table 6**.



376

377 **Fig. 16.** Mean mechano-sorptive strain (ϵ_{ms}) and associated standard deviations on the compression face of unreinforced and
 378 reinforced beams

379

380 At week 7, there is a 9.0% difference when comparing the mechano-sorptive creep strain on the compression face of Group

381 UV and Group RV. The percentage difference increases throughout the test period to a maximum of 24.4% after 71 weeks.

382 Although there is a large percentage difference between the mean results of the unreinforced and reinforced beam groups,

383 the difference is not statistically significant at any time during the test.

384 **Table 6.** Comparison between the mean (standard deviation) mechano-sorptive strain (ϵ_{ms}) on the compression side of
 385 unreinforced and reinforced beams ($\mu\epsilon$)

Strain ($\mu\epsilon$)	Week 7	Week 15	Week 31	Week 47	Week 55	Week 71
Unreinforced	-303.96 (113.25)	-354.10 (117.36)	-433.09 (155.21)	-443.52 (176.59)	-465.90 (182.87)	-466.21 (194.28)
Reinforced	-277.85 (62.27)	-307.26 (86.28)	-361.13 (108.88)	-359.75 (120.87)	-373.92 (123.32)	-364.97 (124.45)
Percentage Diff.	9.0%	14.2%	18.1%	20.9%	21.9%	24.4%
Student's t-test	Not Sig.	Not Sig.	Not Sig.	Not Sig.	Not Sig.	Not Sig.
p-Value	0.603	0.411	0.335	0.321	0.291	0.268

386

387 This shows that despite FRP reinforcement, there is similar mechano-sorptive creep behaviour in the unreinforced and

388 reinforced beams loaded to a common bending stress and subjected to the same changes in moisture content. This finding

389 demonstrates that for the test geometry studied and the FRP reinforcement utilised, the stress level in the timber is the main

390 driver of the mechano-sorptive creep behaviour. This influence of different FRP types and percentage area reinforcement

391 should be investigated to see if this finding applies more generally.

392 4 Summary and Conclusion

393 Matched groups of unreinforced glued laminated beams and glued laminated beams reinforced with NSM Basalt FRP

394 reinforcement have been subjected to long-term creep tests in a controlled variable climate. The creep tests confirm that

395 reinforcing timber with an FRP material of superior properties has a positive effect on the creep behaviour of timber in a

396 variable climate. The following conclusions can be formulated based on the investigation presented:

397 • Due to the BFRP reinforcement, the mean deflection of the reinforced beams were found to be significantly less

398 than that of the unreinforced beams when subjected to a common maximum compressive stress and variable

399 climate. Mean relative creep results demonstrated that the difference is statistically significant after just the first
400 relative humidity cycle. The BFRP reinforcement also resulted in more consistent deflection behaviour in FRP
401 reinforced beams thereby increasing the reliability of such elements when predicting long-term deflections.

- 402 • A statistically significant reduction in the total creep strain was measured on the tension face of reinforced
403 beams due to the BFRP reinforcement. As expected, for the total creep strains measured on the compression
404 face, there was found to be a statistically insignificant difference.
- 405 • Swelling and shrinkage tests have shown that the superior stiffness of the BFRP rod reinforcement restrains the
406 timber in the tensile zone under changing relative humidity conditions, resulting in reduced hygro-mechanical
407 response or swelling/shrinkage strain in the reinforced beams.
- 408 • Utilising matched groups, the mechano-sorptive strain component has been characterised for unreinforced and
409 reinforced beams. The results have shown that the BFRP reinforcement has a statistically insignificant impact
410 on the mechano-sorptive strain on the compression and tension faces.
- 411 • A reduced hygro-mechanical response on the tension face of the reinforced beams was observed. The BFRP
412 rod reinforcement restricts the tensile lamination from swelling or shrinking and results in a reduced
413 swelling/shrinkage strain.

414
415 The reduced creep deflection of the reinforced beam group, observed in this as well as other studies reported in the
416 literature, cannot be attributed to a reduced mechano-sorptive creep response but is in fact due to a reduction in the
417 swelling/shrinkage response due to the addition of FRP material of greater stiffness. These findings present the potential
418 to describe the long-term deflection of FRP reinforced timber elements through short-term tests on the swelling/shrinkage
419 behaviour of the reinforced section. While these observations are valid for the current test set-up, additional tests are
420 required to confirm its validity as the influence of timber species, FRP type, reinforcement percentage and the applied
421 stress level also influence the creep behaviour and must be examined. The creep results presented in this study, and those
422 from tests performed in a constant climate [24], can be used to validate a hygro-mechanical numerical model to predict the
423 creep behaviour of unreinforced and reinforced timber elements. A validated numerical model will allow various FRP
424 types, reinforcement percentages to be examined in addition to examining the influence of stress level on the creep
425 behaviour.

426 Acknowledgments 427

428 This work has been carried out as part of the project 'Innovation in Irish timber Usage' (Project Ref. 11/C/207) funded by
429 the Department of Agriculture, Food and the Marine of the Republic of Ireland under the FIRM/RSF/COFORD scheme.

430 The authors would also like to thank ECC Ltd. (Earrai Coillte Chonnacht Teoranta) for supplying all the timber used in
431 this project. The contribution of the technical staff of the College of Engineering and Informatics, NUIG, in particular,
432 Peter Fahy, Colm Walsh and Gerard Hynes, is gratefully acknowledged.

433 References

- 434 [1] Schober K-U, Harte AM, Kliger R, Jockwer R, Xu Q, Chen J-F. FRP reinforcement of timber structures. *Constr*
435 *Build Mater* 2015;97:106–18. doi:10.1016/j.conbuildmat.2015.06.020.
- 436 [2] Kliger IR, Haghani R, Brunner M, Harte AM, Schober K-U. Wood-based beams strengthened with FRP laminates:
437 improved performance with pre-stressed systems. *Eur J Wood Wood Prod* 2016;74:319–30. doi:10.1007/s00107-
438 015-0970-5.
- 439 [3] Gilfillan JR, Gilbert SG, Patrick GRH. The improved performance of home grown timber glulam beams using
440 fibre reinforcement. *J Inst Wood Sci* 2001;15:307–17.
- 441 [4] Raftery G, Harte A. Low-grade glued laminated timber reinforced with FRP plate. *Compos Part B Eng*
442 2011;42:724–35. doi:10.1016/j.compositesb.2011.01.029.
- 443 [5] Franke S, Franke B, Harte AM. Failure modes and reinforcement techniques for timber beams – State of the art.
444 *Constr Build Mater* 2015;97:2–13. doi:10.1016/j.conbuildmat.2015.06.021.
- 445 [6] O’Neill C, McPolin D, Taylor SE, Harte AM, O’Ceallaigh C, Sikora KS. Timber moment connections using glued-
446 in basalt FRP rods. *Constr Build Mater* 2017;145:226–35. doi:10.1016/j.conbuildmat.2017.03.241.
- 447 [7] Borri A, Corradi M, Grazini A. A method for flexural reinforcement of old wood beams with CFRP materials.
448 *Compos Part B Eng* 2005;36:143–53. doi:http://dx.doi.org/10.1016/j.compositesb.2004.04.013.
- 449 [8] De la Rosa García P, Escamilla AC, Nieves González García M. Bending reinforcement of timber beams with
450 composite carbon fiber and basalt fiber materials. *Compos Part B Eng* 2013;55:528–36.
451 doi:10.1016/j.compositesb.2013.07.016.
- 452 [9] Raftery G, Harte A. Nonlinear numerical modelling of FRP reinforced glued laminated timber. *Compos Part B-
453 Engineering* 2013;52:40–50. doi:10.1016/j.compositesb.2013.03.038.
- 454 [10] Thorhallsson ER, Hinriksson GI, Snæbjörnsson JT. Strength and stiffness of glulam beams reinforced with glass
455 and basalt fibres. *Compos Part B Eng* 2017;115:300–7. doi:10.1016/j.compositesb.2016.09.074.
- 456 [11] Harte AM, Dietsch P. Reinforcement of timber structures: A state-of-the-art report. Shaker Verlag GmbH,
457 Germany; 2015.

- 458 [12] Brunetti M, Christovasilis IP, Micheloni M, Nocetti M, Pizzo B. Production feasibility and performance of carbon
459 fibre reinforced glulam beams manufactured with polyurethane adhesive. *Compos Part B Eng* 2018;156:212–9.
460 doi:10.1016/j.compositesb.2018.08.075.
- 461 [13] Lorenzis L De, Scialpi V, La Tegola A. Analytical and experimental study on bonded-in CFRP bars in glulam
462 timber. *Compos Part B Eng* 2005;36:279–89. doi:10.1016/j.compositesb.2004.11.005.
- 463 [14] De la Rosa García P, Cobo Escamilla A, González García MN. Analysis of the flexural stiffness of timber beams
464 reinforced with carbon and basalt composite materials. *Compos Part B Eng* 2016;86:152–9.
465 doi:10.1016/j.compositesb.2015.10.003.
- 466 [15] Brady JF, Harte AM. Prestressed FRP flexural strengthening of softwood glue-laminated timber beams. Proc. 2008
467 World Conf. Timber Eng., Miyazaki, Japan: 2008.
- 468 [16] CEN. EN 1995-1-1. Eurocode 5: Design of timber structures - Part 1-1: General - Common rules and rules for
469 buildings. Comité Européen de Normalisation, Brussels, Belgium; 2005.
- 470 [17] Senft J, Suddarth S. An analysis of creep-inducing stress in Sitka spruce. *Wood Fiber Sci* 1971;2:321–7.
- 471 [18] Toratti T. Creep of timber beams in a variable environment. Laboratory of Structural Engineering and Building
472 Physics, Helsinki University of Technology, Finland, 1992.
- 473 [19] Davidson RW. The influence of temperature on creep in wood. *For Prod J* 1962;12:377–81.
- 474 [20] Hering S, Niemz P. Moisture-dependent, viscoelastic creep of European beech wood in longitudinal direction. *Eur*
475 *J Wood Wood Prod* 2012;70:667–70. doi:10.1007/s00107-012-0600-4.
- 476 [21] Plevris N, Triantafillou T. Creep behavior of FRP-reinforced wood members. *J Struct Eng* 1995;121:174–86.
477 doi:10.1061/(ASCE)0733-9445(1995)121:2(174).
- 478 [22] Yahyaei-Moayyed M, Taheri F. Creep response of glued-laminated beam reinforced with pre-stressed sub-
479 laminated composite. *Constr Build Mater* 2011;25:2495–506. doi:10.1016/j.conbuildmat.2010.11.078.
- 480 [23] O’Ceallaigh C, Sikora K, McPolin D, Harte AM. Viscoelastic Creep in Reinforced Glulam. Proc. 2016 World
481 Conf. Timber Eng., Vienna, Austria: 2016.
- 482 [24] O’Ceallaigh C, Sikora K, McPolin D, Harte AM. An investigation of the viscoelastic creep behaviour of basalt
483 fibre reinforced timber elements. *Constr Build Mater* 2018;187:220–30. doi:10.1016/j.conbuildmat.2018.07.193.
- 484 [25] Armstrong LD, Kingston RS. Effect of moisture changes on creep in wood. *Nature*, London 1960;185:862–3.
485 doi:10.1038/185862c0.

- 486 [26] Toratti T. Modelling the Creep of Timber Beams. *J Struct Mech* 1992;25:12–5.
- 487 [27] Lu JP, Leicester RH. Mechano-sorptive effects on timber creep. *Wood Sci Technol* 1997;31:331–5.
488 doi:10.1007/BF01159152.
- 489 [28] Toratti T, Svensson S. Mechano-sorptive experiments perpendicular to grain under tensile and compressive loads.
490 *Wood Sci Technol* 2000;34:317–26. doi:10.1007/s002260000059.
- 491 [29] Bengtsson C. “Short-term” mechano-sorptive creep of well-defined spruce timber. *Holz Als Roh-Und Werkst*
492 2001;59:117–28. doi:10.1007/s001070050483.
- 493 [30] Bengtsson C, Kliger R. Bending creep of high-temperature dried spruce timber. *Holzforschung* 2003;57:95–100.
494 doi:10.1515/hf.2003.015.
- 495 [31] Srpčič S, Srpčič J, Saje M, Turk G. Mechanical analysis of glulam beams exposed to changing humidity. *Wood*
496 *Sci Technol* 2009;43:9–22. doi:10.1007/s00226-008-0196-3.
- 497 [32] Ormarsson S, Dahlblom O. Finite element modelling of moisture related and visco-elastic deformations in
498 inhomogeneous timber beams. *Eng Struct* 2013;49:182–9. doi:http://dx.doi.org/10.1016/j.engstruct.2012.10.019.
- 499 [33] Hunt DG. Limited mechano-sorptive creep of beech wood. *J Inst Wood Sci* 1982;9:136–8.
- 500 [34] Zhou Y, Fushitani M, Kubo T, Ozawa M. Bending creep behavior of wood under cyclic moisture changes. *J Wood*
501 *Sci* 1999;45:113–9. doi:10.1007/BF01192327.
- 502 [35] Runyen RW, Dinehart DW, Gross SP, Dunn WG. Creep behavior of wood I-joists with web openings exposed to
503 normal and low relative humidity conditions. *Proc. World Conf. Timber Eng. WCTE 2010, June 20 - June 24,*
504 *Trento, Italy: 2010.*
- 505 [36] Fortino S, Hradil P, Genoese A, Genoese A, Pousette A. Numerical hygro-thermal analysis of coated wooden
506 bridge members exposed to Northern European climates. *Constr Build Mater* 2019;208:492–505.
507 doi:10.1016/j.conbuildmat.2019.03.012.
- 508 [37] Bengtsson C. Mechano-sorptive bending creep of timber - influence of material parameters. *Holz Als Roh-Und*
509 *Werkst* 2001;59:229–36. doi:10.1007/s001070100217.
- 510 [38] Abdul-Wahab HMS, Taylor GD, Price WF, Pope DJ. Measurement and modelling of long-term creep in glued
511 laminated timber beams used in structural building frames. *Struct Eng* 1998;76:271–82.
- 512 [39] Gilfillan JR, Gilbert SG, Patrick GRH. The use of FRP composites in enhancing the structural behavior of timber
513 beams. *J Reinf Plast Compos* 2003;22:1373–88. doi:10.1177/073168403035583.

- 514 [40] Kliger R, Al-Emrani M, Johansson M, Crocetti R. Strengthening timber with CFRP or steel plates - Short and long-
515 term performance. Proc. 10th World Conf. Timber Eng. 2008, June 2 - June 5, vol. 1, Miyazaki, Japan: 2008, p.
516 414–21.
- 517 [41] Raftery G, Harte A. Material characterisation of fast-grown plantation spruce. Struct Build 2014;167:380–6.
518 doi:10.1680/stbu.12.00052.
- 519 [42] CEN. EN 408. Timber structures - Structural timber and glued laminated timber - Determination of some physical
520 and mechanical properties. Comité Européen de Normalisation, Brussels, Belgium: 2012.
- 521 [43] MagmaTech Limited. Rockbar-Corrosion resistant basalt fibre reinforcing bars. Tech Data Sheet, Accessed,
522 11/10/2014 2014.
- 523 [44] ISO. 10406-1. Fibre-reinforced polymer (FRP) reinforcement of concrete Test methods Part 1: FRP bars and grids.
524 ISO, Geneva, Switzerland; 2015.
- 525 [45] O’Ceallaigh C. An Investigation of the Viscoelastic and Mechano-sorptive Creep Behaviour of Reinforced Timber
526 Elements. PhD Thesis, National University of Ireland Galway, 2016.
- 527 [46] Ranta-Maunus A, Korttesmaa M. Creep of Timber during Eight Years in Natural Environments. Proc. World Conf.
528 Timber Eng. WCTE 2000, Whistler, British Columbia: 2000.
- 529 [47] O’Ceallaigh C, Sikora K, McPolin D, Harte AM. An Experimental and Numerical Study of Moisture Transport
530 and Moisture-induced Strain in Fast-grown Sitka Spruce. Cienc y Tecnol 2019;21:45–64. doi:10.4067/S0718-
531 221X2019005000105.

532